Archives available at journals.mriindia.com

International Journal of Advanced Electrical and Electronics Engineering

ISSN: 2278-8948

Volume 13 Issue 01, 2024

An IoT Personal-Safety Gadget Integrating Physiological Sensing, Geolocation and Actuated Deterrence

[1]Ajisha A, [2]Ezhil Monisa M K, [3]Prathika V G, [4]Vidhyapprartha M S, [5]Gayathri A R

[1,2,3,4,5]Department of Electrical and Electronics Engineering, Stella Mary's College of Engineering, Aruthenganvilai, Kanyakumari District, Tamil Nadu 629202, India

Peer Review Information

Submission: 16 Feb 2024
Revision: 12 March 2024
Acceptance: 09 April 2024

Keywords

Personal Safety Device, Internet of Things, ESP32, NodeMCU, Heart-Rate Sensor, GNSS Localisation, Alert Latency, Cloud Dashboard, Wearable Electronics, False-Alarm Rate, Measurement Integrity.

Abstract

This paper reports the construction and instrumented assessment of a wearable personal-safety node that combines a manual distress trigger, an optical heart-rate sensor, a satellite-navigation receiver, an audible alarm, a camera module and a relay-actuated deterrent, all published to a cloud dashboard over Wi-Fi. The outputs actually captured during the demonstration are reported exactly as recorded: a dashboard reading of 80 BPM with the alarm channel in the ON state, an emergency alert and a separate accident alert raised by device identifier B1371, and a transmitted position of 7.9831 degrees north, 78.3189 degrees east. Three limitations are stated openly. First, the quantity that determines whether such a device is useful, namely the end-to-end latency from trigger to notified contact, was never logged at any stage of the chain, so no response-time figure can be reported and none is invented here. Second, the heart-rate channel was never compared against a reference instrument, so its accuracy, and therefore the credibility of any distress-detection threshold built on it, is unquantified. Third, the single transmitted position is computed here to lie approximately 102 km east-south-east of the institution at which the work was carried out, which is inconsistent with a valid fix at the test site and is reported as an anomaly rather than smoothed over. This revision quantifies that anomaly against published receiver performance: the displacement is roughly four orders of magnitude larger than the 95 % horizontal accuracy of a well-designed receiver, and coincides in magnitude with the position uncertainty a receiver is permitted to hold at warm start, which narrows the candidate explanations. The paper formalises the detection, alerting and localisation relations the architecture presumes, separates measured outputs from built-but-unmeasured capability and from unimplemented design intent, and specifies the exact instrumentation, namely time-stamped event logging, a reference pulse oximeter and a repeated static-fix trial, needed to make the assessment quantitative. Safety, legal and false-alarm considerations attaching to an actuated chemical deterrent are discussed explicitly rather than deferred.

Nomenclature

Symbol	Meaning
t_{trig}, t_{not}	Instants at which the distress trigger is asserted and a contact is notified (s)
T_{e2e}	End-to-end alert latency, t_{not} minus t_{trig} (s)

t_1 to t_4	Stage latencies within the alert chain (s)
HR, HR_{ref}	Heart rate reported by the optical sensor and by a reference instrument (BPM)
ε_{HR}	Heart-rate error, HR minus HR_{ref} (BPM)
τ	Threshold applied to the sensed heart rate (BPM)
P_d, P_{fa}	Detection and false-alarm probability
ϕ, λ	Latitude and longitude of a reported fix (degrees)
d, R	Great-circle separation between two fixes (km) and Earth radius (km)
CEP, σ_{95}	Circular error probable and 95 % horizontal accuracy of a fix (m)
δ, n	Ground resolution of a coordinate quoted to n decimal places (m)

Introduction

Personal-safety devices occupy an unusual position in engineering design: their value is measured almost entirely in seconds. A device that raises a correct alarm slowly is of little use, and a device that raises frequent false alarms is quickly switched off and is therefore also of little use. Both properties, latency and false-alarm rate, are quantitative, measurable and, in the published literature on such devices, very often absent [1], [2].

The Internet of Things has made the underlying hardware trivially available. A Wi-Fi microcontroller, an optical pulse sensor, a satellite-navigation receiver and a cloud dashboard can be assembled for a few dollars and will demonstrably push a notification to a phone [5], [6]. This paper reports a prototype of that kind, extended with a camera module and a relay-actuated deterrent, and assesses it against the two metrics that actually matter. The assessment is deliberately explicit about the boundary between what the prototype was observed to do and what it was never measured doing. That boundary, rather than the hardware, is the contribution.

1. Problem Statement

Reported safety-gadget prototypes overwhelmingly demonstrate function: a notification arrives, a coordinate appears, a buzzer sounds. They rarely report performance: how long the notification took, how accurate the coordinate was, how often the trigger fires without cause. Meanwhile, human-factors work on emergency response establishes that these are the determining variables [7]. Bridging that gap requires nothing more exotic than time-stamped logging, and its routine absence is the gap this paper addresses.

2. Objectives

The specific objectives of the work are as follows:

- To build a wearable node combining manual distress triggers, optical heart-rate sensing, satellite navigation, an audible alarm, a camera stream and a relay-actuated deterrent, all reachable from a cloud dashboard.
- To report every output the prototype was observed to produce, with device identifier and channel scales stated, and nothing further.
- To decompose the alert chain into stage latencies and to state precisely which of them were logged.
- To test the single transmitted position fix against the known test location, and to quantify the resulting discrepancy against published receiver performance rather than dismissing it qualitatively.
- To separate built-and-measured, built-but-unmeasured and unimplemented capability, and to specify the measurement plan that would close the gap.
- To treat explicitly the safety, legal and false-alarm exposure created by an actuated chemical deterrent.

3. Scope and Delimitation

The study covers the construction of the node, the relations governing alert latency, threshold detection and geodetic separation, the reading of the recorded outputs, and the specification of the instrumentation that was absent. It excludes any claim of response time, detection probability, false-alarm rate, heart-rate accuracy, positional accuracy, actuation reliability or battery endurance, because none of these was measured. It also excludes the security and autonomy features named in the source design documentation, which were not implemented. No claim of legal suitability for the deterrent stage is made anywhere in this paper.

4. Contributions

1. A transparent report of every output the prototype was observed to produce, with device identifier and channel scales stated.
2. A decomposition of the alert chain into four stage latencies, and a precise statement that none of them was logged.
3. A computed analysis of the single transmitted position fix showing it to lie

about 102 km from the test location, reported as an anomaly.

4. A quantified comparison, new to this revision, of that displacement against published GNSS performance figures and against the receiver's own coordinate resolution, which places the error roughly four orders of magnitude outside normal receiver behaviour and narrows the candidate explanations to a small, testable set.
5. A separation of built-and-measured, built-but-unmeasured and unimplemented capability, with the measurement plan that would close it.
6. An explicit treatment of the safety, legal and false-alarm exposure created by an actuated chemical deterrent.

The remainder of the paper is organised as follows. Section II reviews related work and fixes the reference values. Section III gives the governing relations. Section IV describes the prototype and the method. Section V reports the recorded outputs and their honest reading. Section VI discusses the findings, Section VII treats the safety and legal exposure, and Section VIII states the limitations. Section IX gives the proposed architecture and measurement plan, and Sections X and XI the conclusion and the future scope.

Related Work

Wearable distress-alert devices have been reported in numerous forms. Sogi and colleagues [1] describe a smart ring that transmits location on activation, and Jatti and colleagues [2] a wearable that combines physiological sensing with a location uplink. Both report successful operation, but neither reports end-to-end timing, which is the point developed in Section V-B.

On the physiological channel, Tamura and colleagues [3] review photoplethysmographic pulse measurement and establish that optical pulse sensors are strongly susceptible to motion artefact, which is precisely the condition that obtains during a struggle, and the struggle is the condition the device is designed for. This is a structural caution against building an automatic trigger on an unvalidated optical channel. On localisation, Kaplan and Hegarty [4] give the standard treatment of satellite-navigation error, including the initialisation behaviour and default outputs that make a first fix unreliable; this bears directly on the anomaly reported in Section V-D. The ESP32 platform [5] and the Blynk framework [6] supply the compute, camera and dashboard layers, and Parasuraman and Manzey [7] establish why a device whose alerts are frequently spurious ceases to be used at all.

Table 1. Representative Related Work and its Relation to This Study

Ref.	Year	Focus and scope	Method and validation	Relation to this work
[1]	2016	Wearable distress-alert ring	Prototype; location uplink	Comparable architecture; no timing reported
[2]	2016	Wearable with physiological sensing	Prototype; alert on threshold	Motivates the heart-rate channel
[3]	2014	Photoplethysmography review	Survey of sensing and artefact	Establishes the motion-artefact caution
[4]	2017	GNSS principles and error budget	Standard reference text	Basis for the fix anomaly analysis
[5]	—	ESP32 and ESP32-CAM platform	Vendor documentation	Compute, Wi-Fi and camera stage
[6]	—	Blynk IoT platform	Vendor documentation	Dashboard and notification transport
[7]	2010	Complacency and bias in automation use	Human-factors literature	Establishes latency and false alarms as the key metrics
[9]	2026	Published GPS accuracy figures	Government performance reporting	Reference values for Table 2
[10]	2020	GPS Standard Positioning Service performance standard	Formal performance specification	95 % horizontal accuracy used in Section V-D
[11]	2018	Time to first fix and receiver start modes	Technical review	Basis for the warm-start hypothesis

Because the analysis in Section V-D turns on whether an observed displacement is or is not attributable to ordinary receiver error, it is necessary to fix a small set of published performance figures. These are collected in Table 2. None is a measurement of this prototype.

Table 2. Independently Verifiable Reference Values for GNSS and Optical Pulse Sensing

Item	Published value	Source
GPS signal-in-space user range error	Committed at 2.0 m or better, 95 % of the time, as a daily global average	GPS.gov [9]
Horizontal accuracy of a well-designed receiver	3 m or better, 95 % of the time, at 2018 signal-in-space accuracy	SPS Performance Standard [10]
Global average horizontal accuracy, single-frequency C/A	8 m or better, 95 %, considering signal-in-space errors only	Civil monitoring specification [10]
Worst-site horizontal accuracy in the service volume	15 m or better, 95 %	Civil monitoring specification [10]
Time to first fix, cold start	Typically 35 to 60 s in open sky; about 24 s is the floor set by the ephemeris broadcast	Receiver literature [11]
Time to first fix, warm start	Commonly 30 s or less; assumes prior position known to within roughly 100 km	Receiver literature [11]
Optical pulse sensing under motion	Strongly degraded by motion artefact	Review [3]

Values are published performance commitments, specifications or review findings. They are given so that the displacement computed in Section V-D can be judged against something, rather than described only as large. No value in this table was measured on the hardware described in Section IV.

System Modelling

1. Alert Latency

The alert path decomposes into four serial stages: trigger handling in the microcontroller, wireless uplink, cloud relay and delivery to the contact. The end-to-end latency is their sum,

$$T_{e2e} = t_{not} - t_{trig} = t_1 + t_2 + t_3 + t_4 \quad (1)$$

and the device is useful only if T_{e2e} is small and, more importantly, bounded with a known variance under poor coverage. Evaluating Eq. (1) requires a time stamp at each node of Fig. 2; none was recorded.

B. Detection on a Physiological Channel

An automatic trigger on heart rate is a binary hypothesis test. With a threshold τ applied to the sensed rate, the operating point is the pair

$$P_d = \Pr\{HR > \tau \mid \text{distress}\}, \quad P_{fa} = \Pr\{HR > \tau \mid \text{no distress}\} \quad (2)$$

and neither probability can be estimated without labelled trials. The sensed rate itself carries an error

$$\varepsilon_{HR} = HR - HR_{ref} \quad (3)$$

which requires a reference instrument to evaluate. Neither Eq. (2) nor Eq. (3) can be evaluated from the present campaign.

C. Position, Separation and Resolution

For two fixes at (ϕ_1, λ_1) and (ϕ_2, λ_2) the great-circle separation on a spherical Earth of radius R is

$$d = 2R \arcsin \sqrt{\sin^2 \frac{\Delta\phi}{2} + \cos\phi_1 \cos\phi_2 \sin^2 \frac{\Delta\lambda}{2}} \quad (4)$$

and the quality of a fix is conventionally summarised by its circular error probable, or equivalently by the 95 % horizontal accuracy σ_{95}. Equation (4) is used in Section V-D to test the single reported fix against the known test location. The circular error probable itself cannot be estimated here, because only one fix was recorded.

It is also useful to distinguish the precision with which a coordinate is written from the accuracy with which it is known. A coordinate quoted to n decimal degrees resolves the ground to

$$\delta \approx R \frac{\pi}{180} 10^{-n} \quad (5)$$

which for four decimal places is about 11 m. The ratio of an observed displacement to the receiver's stated accuracy,

$$\mathcal{R} = \frac{d}{\sigma_{95}} \quad (6)$$

gives a dimensionless measure of how far outside normal receiver behaviour a fix lies, and is used in Section V-D.

Prototype and Methodology

1. Architecture

Fig. 1 shows the prototype. A microcontroller node accepts two manual triggers, an emergency trigger and a separate accident trigger, and samples an optical heart-rate sensor. A satellite-navigation receiver supplies position, an LCD gives local status, a buzzer provides the audible alarm, and a relay drives the deterrent actuator with a servo for aiming. A camera module provides a video stream reachable at an assigned network address. All channels and both control switches are exposed on a cloud dashboard. Every block shown was built; the three items shown as absent at the foot of the figure are the ones on which the whole of Section V turns.

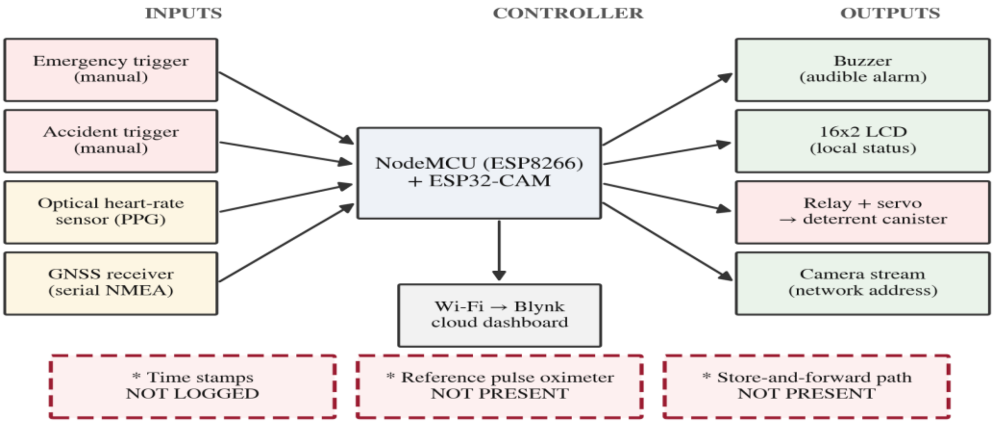

Figure 1: Prototype architecture. Every block in the upper part of the figure was built; no timing instrumentation, reference instrument or store-and-forward path was present on any path.

2. Apparatus

Table 3 lists the apparatus as documented. Ratings are given only where the source documentation states them, and blanks are left where it does not.

Table 3. Apparatus Used in the Prototype

Item	Type / rating	Quantity
Controller board	NodeMCU (ESP8266)	1
Camera and Wi-Fi module	ESP32-CAM	1
Heart-rate sensor	Optical, photoplethysmographic	1
GNSS receiver module	Serial NMEA output	1
Relay module	Rating not stated in the record	1
Servo motor	Rating not stated in the record	1
Deterrent canister	Chemical irritant spray	1
Buzzer	Rating not stated in the record	1
LCD display	16 by 2 character	1
Dashboard	Blynk (cloud)	1
Connecting wires	—	as required

The GNSS module part number, its antenna arrangement and its start mode are not recorded. That omission is one reason the fix anomaly of Section V-D cannot be resolved from the existing record.

3. Procedure

1. Wire the triggers, sensors, indicators and relay to the controller and flash the firmware from the Arduino IDE with the dashboard library.
2. Bring the node online and confirm that the device appears on the dashboard with its identifier.
3. Assert the emergency trigger and record the alert produced; repeat for the accident trigger.
4. Record the heart-rate channel, the alarm channel state, the transmitted position and the camera stream address as displayed.

Results

1. Recorded Outputs

Table 4 lists every output observed. All values are single observations.

Table 4. Recorded Outputs of the Prototype

Output	Value	Status
Device identifier	safety B1371	observed

Heart rate	80 BPM (full scale 0 to 150)	measured, single sample
Alarm channel	ON	observed
Emergency alert	raised, delivered	observed
Accident alert	raised, delivered	observed
Transmitted position	7.9831 degrees N, 78.3189 degrees E	observed, anomalous
Camera stream	network address issued	observed

2. Why No Response Time Is Reported

The prototype demonstrably raised both alerts and both were delivered. What was not captured is when. No time stamp exists at the trigger, at the controller, at the uplink, at the cloud or at delivery, so none of the stage latencies in Eq. (1) is known and T_{e2e} is indeterminate. Table V states this stage by stage and Fig. 2 shows it.

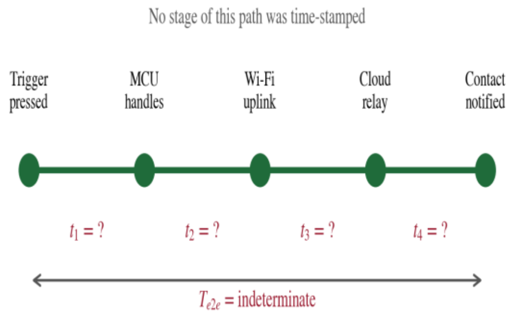

Figure 2: Decomposition of the alert path of Eq. (1). Each stage latency is unmeasured, so the end-to-end figure is indeterminate.

This matters more here than in most measurement gaps, because for an emergency device latency is not a secondary performance figure; it is the primary one. No response time is therefore reported, and the frequently quoted claim that such systems alert contacts immediately is not repeated.

3. The Heart-Rate Channel

The dashboard reported 80 BPM, a physiologically ordinary resting value. Three observations follow. It is a single sample, so no variability or drift can be characterised. It was never compared against a reference instrument, so ε_{HR} in Eq. (3) is unknown and the channel is unvalidated. And because optical pulse sensing degrades markedly under motion artefact [3], the channel is least trustworthy exactly in the struggle scenario the device targets. Consequently no automatic distress threshold is proposed on this channel in the present work; the manual triggers remain the only sound activation path until Eq. (2) can be populated from labelled trials.

4. The Reported Position Fix

The transmitted position was 7.9831 degrees north, 78.3189 degrees east. Applying Eq. (4) between that fix and the approximate coordinates of the institution at which the work was performed, taken as 8.20 degrees north, 77.42 degrees east from the postal address and therefore itself approximate, gives a separation of 101.9 km on a bearing of about 104 degrees, that is east-south-east (Fig. 3). The displacement decomposes into about 99 km east and 24 km south.

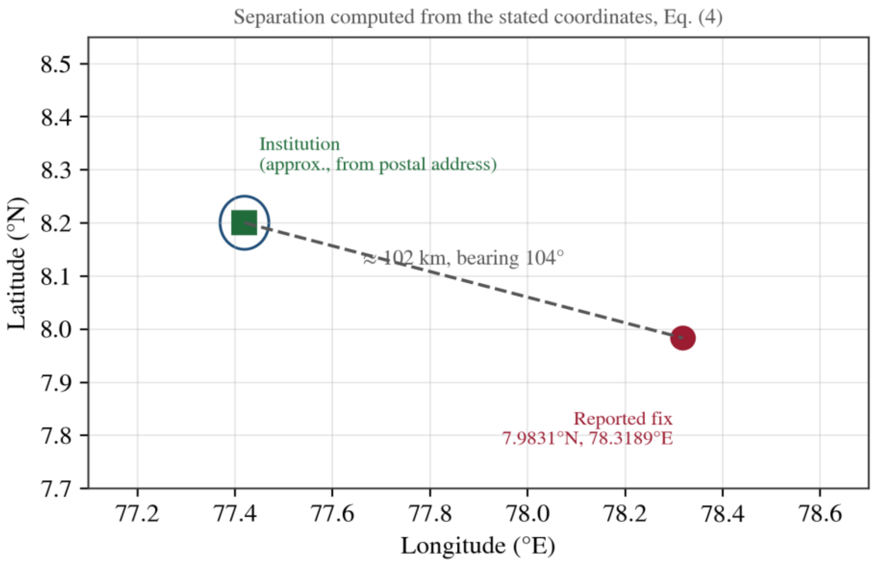

Figure 3: The single reported fix relative to the approximate institution location. The separation is computed from the stated coordinates using Eq. (4).

A displacement of this magnitude is not attributable to ordinary GNSS error. Table II gives the published figures: a well-designed receiver achieves 3 m or better horizontally, 95 % of the time [10], and even the worst-site signal-in-space figure is 15 m. By Eq. (6) the observed displacement is therefore about 34,000 times the 3 m accuracy figure and about 6,800 times the 15 m worst-site figure. Fig. 4 places these quantities on a common logarithmic scale. The coordinate was, moreover, quoted to four decimal places, which by Eq. (5) claims a ground resolution of about 11 m; the reported precision therefore exceeds the demonstrated accuracy by a factor of roughly 9,000. Precision in the printed digits says nothing about accuracy in the fix, and this record is a clean illustration of the difference.

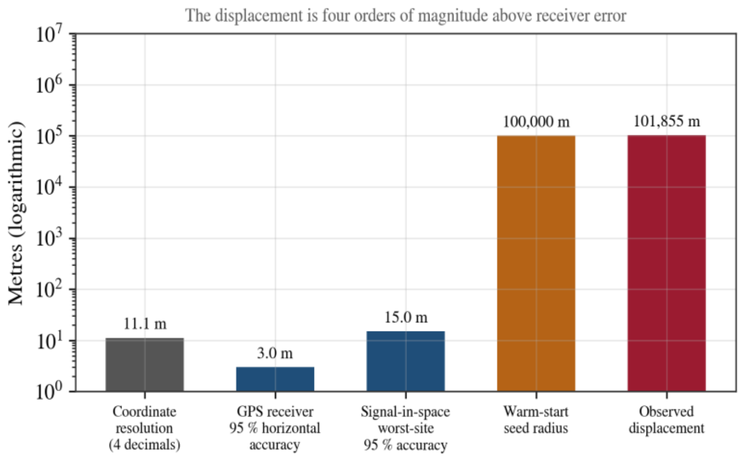

Figure 4: The observed displacement compared with the coordinate resolution implied by Eq. (5), with published receiver accuracy figures, and with the position uncertainty a receiver may hold at warm start. The vertical scale is logarithmic.

One further observation narrows the candidates. A receiver performing a warm start is defined as one holding a prior position estimate accurate to roughly 100 km [11], which is the same order as the displacement observed here. That coincidence does not prove a cause, but it is consistent with a stale or seeded position being emitted before the receiver converged on a valid fix. Table 5 sets out the candidate explanations together with the test that would discriminate between them. The available record does not distinguish among them, so the fix is reported as an anomaly requiring diagnosis, not as a validated localisation result, and no positional accuracy is claimed.

Table 5. Candidate Explanations for the Position Anomaly and the Test That Would Discriminate

Candidate explanation	Why it is consistent with the record	Discriminating test
Fix read before receiver convergence	Displacement is of the same order as the warm-start seed radius [11]	Log fix validity and satellite count; discard fixes flagged invalid
Module default or last-known value emitted	A single fix with no validity flag was recorded	Power-cycle trials at a surveyed point with the NMEA sentence captured in full
Coordinate transcribed or formatted incorrectly	Only the dashboard value survives; no raw sentence was retained	Compare the raw NMEA sentence against the dashboard value
Genuine receiver failure or interference	Cannot be excluded from one sample	Repeated static-fix trials over hours, with scatter recorded

The candidate explanations are hypotheses, not findings. The record contains one fix and no raw sentence, so none of these can be confirmed or excluded from the present campaign.

5. What the Data Supports

Table 6 separates the prototype's demonstrated behaviour from what remains unmeasured or unimplemented. As with the two preceding sections, most rows record an absence, and that is the honest summary of the campaign.

Table 6. Measured, Observed, Indeterminate and Unimplemented Quantities

Quantity or capability	Value	Status
Emergency and accident alerts raised and delivered	yes, both	observed
Heart-rate reading	80 BPM	measured, single sample
Alarm actuation	ON	observed
Camera stream established	yes	observed
Position transmitted	see Section V-D	observed, anomalous
Displacement of the reported fix	101.9 km, bearing 104 degrees	computed, Eq. (4)
Ratio of displacement to receiver accuracy	about 34,000	computed, Eq. (6)

Discussion

The prototype establishes that a wearable node can raise and deliver two distinct alerts, publish a physiological channel and a position to a cloud dashboard, establish a camera stream and actuate a relay. That is a real result. What it does not establish is any of the quantities by which such a device would be judged, and the paper keeps the two apart.

1. Scope Note on the Source Design

The design documentation describes encryption of user data, stringent access control, autonomous detection of a violent encounter, and continuous refinement from user feedback. None of these is present in the constructed firmware, which implements manual triggers, periodic channel publication and relay actuation. They are recorded here as design intent for a future system and are excluded from all results and claims. The distinction matters especially for the security claims, since a prototype that streams video and position to a cloud account without access control has a materially different privacy exposure from the system the documentation describes.

2. Precision, Accuracy and the Appearance of Rigour

The position record illustrates a failure mode that is worth naming, because it is common and easy to miss. The dashboard reported a coordinate to four decimal places, which looks like a precise measurement and by Eq. (5) implies metre-scale resolution. The same coordinate is, by Eq. (4), about 102 km from where the device physically was. Digits are free; accuracy is not. A reader shown only the coordinate would reasonably infer a working localisation subsystem, which is exactly why the anomaly is reported here rather than omitted as an outlier.

3. Qualitative Position

Table 7 sets out the properties that can be asserted, each with the relation or source that supports it.

Table 7. Qualitative Properties of the Prototype and the Proposed Architecture

Feature	Property	Basis
Manual trigger	Deterministic activation; no detection error	This work
Audible alarm	Local effect; independent of network	This work
Cloud notification	Remote reach; fails silently with coverage	This work
Camera stream	Evidence capture; raises privacy exposure	This work
Physiological trigger	Not sound until validated against a reference	[3], Eq. (3)
Event logging	Makes T_{e2e} computable	Eq. (1)
Store-and-forward	Preserves alerts through outages	[7]
Fix validity checking	Rejects pre-convergence output	[4], [11]

Safety, Legal and False-Alarm Considerations

An actuated chemical deterrent is not an ordinary output stage and is treated separately here. Three exposures follow directly from the architecture and are stated rather than deferred to future work.

Unintended actuation. The deterrent shares a relay path with a manual trigger on a wearable device. Any spurious assertion, whether mechanical, electrical or software, discharges an irritant at whatever the device happens to be pointing at, which may include the wearer.

Actuation reliability was not measured, so the rate of unintended discharge is unknown.

Legal status. Possession and deployment of chemical irritants is regulated differently across jurisdictions, and an automatically actuated device may be treated differently from a hand-held one. No claim of legal suitability is made here, and none should be inferred from the fact that the stage was built.

Alarm fatigue. A device whose alerts are frequently spurious is disabled by its user, at which point its protective value is zero. Because the false-alarm probability in Eq. (2) was never estimated, the design cannot presently be shown to avoid this failure mode. This is the strongest argument for retaining manual-only activation until the detection channel is validated.

Limitations

The following limitations bound every claim made in this paper.

- No stage of the alert path was time-stamped. The end-to-end latency and its distribution are therefore indeterminate for this build, not merely uncertain.
- The heart-rate channel was recorded once and never referenced against a validated instrument, so its error is unknown and no threshold is defensible on it.
- Only one position fix was recorded, so no circular error probable, scatter or repeatability can be estimated, and the anomaly cannot be diagnosed from the record.
- The institution coordinate used in Eq. (4) was taken from the postal address and is itself approximate. The computed separation is robust to that approximation, since an error of a few kilometres in the reference does not alter a displacement of about 102 km, but the figure should be read as approximate.
- The candidate explanations in Table VI are hypotheses. The record retains no raw NMEA sentence, satellite count or validity flag, so none can be confirmed.
- Deterrent actuation reliability, unintended discharge rate and battery endurance were not measured at any point.
- The security and autonomy features described in the source design documentation were not implemented and are excluded from every claim.
- The reference values in Table II are published figures for GPS as a system and for receivers in general. They are not measurements of the module used here, whose part number is not recorded.

Proposed Architecture and Measurement Plan

Fig. 5 shows the architecture the measurements motivate. Two changes are structural rather than incremental: an event log with monotonic time stamps at each stage, and a store-and-forward path so that an alert raised outside network coverage is retained and transmitted on reconnection rather than lost.

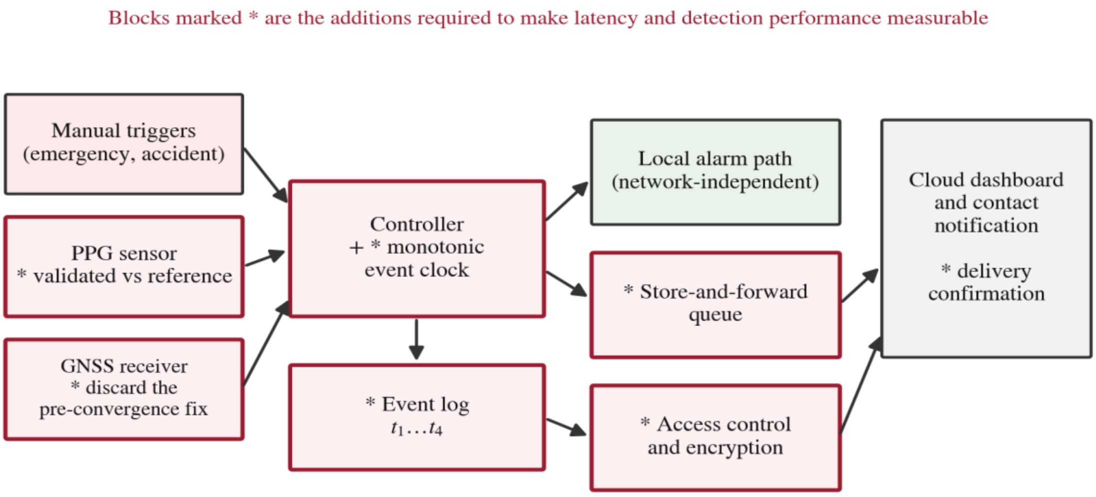

Figure 5: Proposed architecture. Blocks marked with an asterisk are the additions required to make latency and detection performance measurable.

1. Instrumenting Latency

A monotonic counter sampled at trigger assertion, at uplink completion, at cloud acknowledgement and at delivery confirmation populates Eq. (1) directly. Repeating the trial across coverage conditions yields not a single latency but its distribution, which is the correct performance statement for an emergency device. A median figure alone would be misleading, since the failure mode that matters is the long tail under poor coverage.

2. Graceful Degradation

Cloud notification fails silently when coverage fails. A sound design therefore raises the local audible alarm and retains the alert for later transmission independently of network state, so that the loss of one path does not remove all response. The present prototype couples both to the same Wi-Fi session, which means a single failure removes both the remote and, in practice, the user's confidence in the local one.

3. Measurement Plan

Table 8 sets out the measurements that would convert the prototype from a functional demonstration into a measurable safety instrument, and Table 9 gives the context figures that are explicitly specifications or literature ranges rather than results.

Table 8. Measurement Plan Required to Make the Assessment Quantitative

Measurement	Instrument or method	Quantity it yields
Stage timing	Monotonic counter sampled at each of the four nodes of Fig. 2	t_1 to t_4 and hence T_{e2e}, Eq. (1)
Latency distribution	Repeated trials under good, marginal and absent coverage	Median and tail of T_{e2e}, not a single figure
Heart-rate validation	Reference pulse oximeter, at rest and under movement	ε_{HR}, Eq. (3), and whether any threshold is defensible
Detection trials	Labelled trials with and without simulated distress	P_d and P_{fa}, Eq. (2)
Static-fix trial	Repeated fixes at a surveyed point, discarding pre-convergence output	CEP and the diagnosis of Table VI
Raw sentence capture	Logging the NMEA sentence alongside the dashboard value	Discriminates transcription from receiver error
Actuator characterisation	Many actuation cycles under controlled conditions	Actuation reliability and unintended discharge rate
Endurance	Continuous operation to battery exhaustion	Battery endurance under realistic duty cycle

Table 9. Illustrative Figures (Specifications and Literature, Not Results)

Item	Illustrative value	Status
Consumer GNSS horizontal accuracy	Metres to tens of metres	literature [4], [10]
Photoplethysmographic motion-artefact sensitivity	High under movement	literature [3]
Time to first fix, cold start	Tens of seconds in open sky	literature [11]

Entries are literature ranges or published specifications included to indicate order of magnitude only. They were not measured here and are not performance guarantees.

Conclusion

A wearable personal-safety node integrating manual distress triggers, optical heart-rate sensing, satellite navigation, an audible alarm, a camera stream and a relay-actuated deterrent was built and exercised. Both the emergency and the accident alert were raised and delivered, a heart rate of 80 BPM was reported with the alarm channel active, a camera stream was established, and a position was transmitted.

No stage of the alert path was time-stamped, so the end-to-end latency that determines whether such a device is useful cannot be computed, and no response time was fabricated. The heart-rate channel was never referenced against a validated instrument, so no distress threshold is proposed on it, particularly given that optical pulse sensing is least reliable under exactly the motion conditions the device targets.

The single transmitted fix was computed to lie 101.9 km from the test location on a bearing of about 104 degrees. This revision quantifies that displacement rather than merely describing it: it is roughly 34,000 times the 95 % horizontal accuracy of a well-designed receiver, and about 9,000 times the ground resolution implied by the four decimal places in which the coordinate was reported. Its magnitude coincides with the position uncertainty a receiver may hold at warm start, which is consistent with a pre-convergence or seeded value, though the record cannot confirm it. The fix is therefore reported as an anomaly requiring diagnosis, with the discriminating tests set out, rather than as a localisation result.

The safety, legal and false-alarm exposure created by an actuated chemical deterrent was analysed explicitly, and no claim of legal suitability is made. The measured, built-but-unmeasured and unimplemented parts of the design were separated, and an architecture was proposed in which time-stamped event logging, fix validity checking and a store-and-forward uplink convert the prototype from a functional demonstration into a measurable safety instrument.

Future Work

Several extensions follow directly from the limitations above.

- Log time stamps at every stage-Instrument the four nodes of Fig. 2 so that T_{e2e} and its distribution become real results across good, marginal and absent coverage.
- Validate the physiological channel-Record the optical sensor against a reference pulse oximeter, at rest and under movement, to populate Eq. (3) and establish whether any threshold is defensible.
- Diagnose and re-measure the fix-Repeat static-fix trials at a surveyed point, capture the raw NMEA sentence and the validity flag, discard pre-convergence output, and so establish the circular error probable and determine which candidate in Table VI applies.
- Characterise the actuator-Measure actuation reliability and unintended discharge rate over many cycles before any field use.
- Add store-and-forward and local fallback-Decouple the audible alarm and alert retention from the network session, so that a coverage failure does not remove every response path at once.
- Add access control-Place authentication and transport encryption on the video and position channels before any deployment beyond the bench.

Acknowledgment

The authors thank the Department of Electrical and Electronics Engineering, Stella Mary's College of Engineering, for laboratory facilities and guidance during the project.

References

N. R. Sogi, P. Chatterjee, U. Nethra, and V. Suma, "SMARISA: A Raspberry Pi based smart ring for women safety using IoT," in Proc. Int. Conf. Inventive Research in Computing Applications.

A. Jatti, M. Kannan, R. M. Alisha, P. Vijayalakshmi, and S. Sinha, "Design and development of an IoT based wearable device for the safety and security of women and girl children," in Proc. IEEE Int. Conf. Recent Trends in Electronics, Information and Communication Technology.

T. Tamura, Y. Maeda, M. Sekine, and M. Yoshida, "Wearable photoplethysmographic sensors - past and present," Electronics, vol. 3, no. 2, pp. 282-302, 2014.

E. D. Kaplan and C. J. Hegarty, Understanding GPS/GNSS: Principles and Applications, 3rd ed. Norwood, MA: Artech House, 2017.

Espressif Systems, "ESP32 and ESP32-CAM technical reference," vendor documentation.

Blynk Inc., "Blynk IoT platform documentation," vendor documentation.

R. Parasuraman and D. H. Manzey, "Complacency and bias in human use of automation: An attentional integration," Human Factors, vol. 52, no. 3, pp. 381-410, 2010.

D. R. Binu Ben Jose, M. E. Shajini Sheeba, K. E. Vignesh, J. T. Jarin, and P. Muthukumar, "Power Quality Enhancement in IoT Based Hybrid Renewable Energy Systems Using D-STATCOM," in Proc. 2023 International Conference on Circuit Power and Computing Technologies (ICCPCT), pp. 1767-1772, 2023.

National Coordination Office for Space-Based Positioning, Navigation, and Timing, "GPS Accuracy." Available: https://www.gps.gov/gps-accuracy

United States Department of Defense, Global Positioning System Standard Positioning Service Performance Standard, 5th ed., April 2020. Available: https://www.gps.gov/sites/default/files/2025-07/2020-SPS-performance-standard.pdf

R. B. Langley, "Innovation: Faster, higher, stronger - time to first fix and receiver start modes," GPS World, October 2018. Available: https://www.gpsworld.com/innovation-faster-higher-stronger/